

Notes

Tridentate Coordination of Monosubstituted Derivatives of the Tris(2-pyridylmethyl)amine Ligand to FeCl₃: Structures and Spectroscopic Properties of ((2-Bromopyridyl)methyl)bis(2-pyridylmethyl)amine Fe^{III}Cl₃ and (((2-*p*-Methoxyphenyl)pyridyl)methyl)bis(2-pyridylmethyl)amine Fe^{III}Cl₃ and Comparison with the Bis(2-pyridylmethyl)amine Fe^{III}Cl₃ Complex

Dominique Mandon,* Agathe Nopper,
Thomas Litrol, and Sandrine Goetz

Laboratoire de Chimie Organométallique et de Catalyse,
UMR CNRS No. 7513, Université Louis Pasteur, Institut Le
Bel, 4 rue Blaise Pascal, F-67070 Strasbourg Cedex, France

Received November 28, 2000

Introduction

Small nitrogen tripodal ligands based on alkylpyridyl motifs are known to form stable complexes with a large number of transition metals.¹ Among them, the tris(2-pyridylmethyl)amine ligand (TPA) has been extensively studied because, in part, of the ability of some of its iron complexes to carry out catalytic oxidation reactions similar to those observed with some non-heme metalloenzymes.² The rich bioinspired iron chemistry developed over the past years involves the use of precursors which are in general simple ferric derivatives, alkyl substituted or not.^{3–7} These are compounds for which the standard tetradentate coordination mode of the TPA ligand is observed.^{8,9}

Substituted TPA are known, although at present very little information has been reported about stable ferric monomers of functionalized ligands in that family.^{10–13} We believe that the introduction of functional groups might induce noticeable change in the structure and reactivity of the iron complexes.^{4,14} Thus,

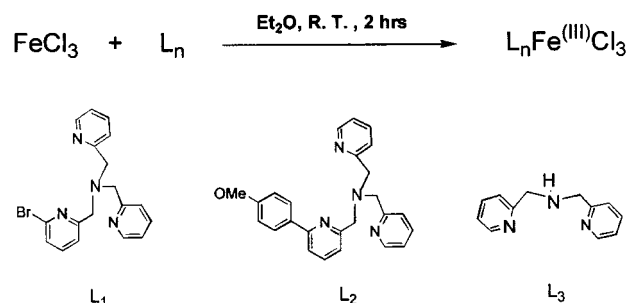


Figure 1. Ligands and complexes reported in this study.

in view of future developments of TPA-based iron systems with functional groups, we have prepared and studied robust chloro-ferric complexes in which the metal is coordinated to a TPA ligand monosubstituted in the α position of one pyridyl arm by a bulky bromine atom or a methoxyphenyl ring. We have found that the steric hindrance provided by the α -substituted arm pushes it away from the coordination site, leaving it free and potentially reactive. We report herein, together with their spectroscopic properties, the crystal structures of the complexes ((2-bromopyridyl)methyl)bis(2-pyridylmethyl)amine Fe^{III}Cl₃, L₁Fe^{III}Cl₃, (((2-*p*-methoxyphenyl)pyridyl)methyl)bis(2-pyridylmethyl)amine Fe^{III}Cl₃, L₂Fe^{III}Cl₃, and a comparison of both spectroscopic and structural features with those of the parent complex bis(2-pyridylmethyl)amine Fe^{III}Cl₃, L₃Fe^{III}Cl₃.

Experimental Section

The UV–vis spectra were recorded on a Varian Cary 05 E UV–vis NIR spectrophotometer. ¹H NMR data were recorded in CD₃CN at ambient temperature on a Bruker AC 300 spectrometer at 300 MHz using the residual signal of CD₂HCN as a reference for calibration.

Ligands L₁ and L₃ were prepared according to published methods.¹⁰ L₂ was prepared from L₁ by adaptation of a published procedure using the Suzuki cross-coupling procedure.¹⁰ ¹H NMR, CDCl₃, δ , ppm, TMS: 8.53, 2H d; 7.95, 2H d; 7.65–7.13 9H m; 6.98, 2H d; 3.96, 4H, s; 3.94, 2H, s; 3.85, 3H, s. Mass spectrum: impact mode, m/z = 396.20. Anal. Calcd for L₂ (C₂₅H₂₄ON₄): C 75.66, H 6.05. Found: C 75.37, H 6.02.

Typical Metalation Experiment. Anhydrous FeCl₃ (0.9 equiv) in dry diethyl ether was added to a solution of ligand L_{*n*} in a diethyl ether. Precipitation occurred immediately, and the reaction medium was allowed to stir for 2 h. The yellow-orange solid was filtered, washed with cold acetonitrile and diethyl ether, and dried under vacuum. Further purification was achieved by diethyl ether crystallization from an acetonitrile solution. The yields are quantitative, and all compounds, air and thermally stable, gave satisfactory elemental analyses.

X-ray Analysis. Quantitative data were obtained at room temperature for L₁Fe^{III}Cl₃ and L₃Fe^{III}Cl₃ and at –100 °C for L₂Fe^{III}Cl₃. All experimental parameters used are given in the Supporting Information. The resulting dataset was transferred to a DEC Alpha workstation, and for all subsequent calculations the Enraf-Nonius OpenMoleN package¹⁸ was used.

- (1) Toftlund, H. *Coord. Chem. Rev.* **1989**, *94*, 67–108.
- (2) Que, L., Jr.; Dong, Y. *Acc. Chem. Res.* **1996**, *29*, 190–196.
- (3) Dong, H.; Fujii, H.; Hendrich, M. P.; Leising, R. A.; Pan, G.; Randall, C. R.; Wilkinson, E. C.; Zang, Y.; Que, L., Jr.; Fax, B. G.; Kauffmann, K.; Münck, E. *J. Am. Chem. Soc.* **1995**, *117*, 2778–2792.
- (4) Lange, S. J.; Miyake, H.; Que, L., Jr. *J. Am. Chem. Soc.* **1999**, *121*, 6330–6331.
- (5) Zheng, H.; Yoo, S. J.; Münck, E.; Que, L., Jr. *J. Am. Chem. Soc.* **2000**, *122*, 3789–3790.
- (6) Ho, R. Y. N.; Roelfes, G.; Hermant, R.; Hage, R.; Feringa, B. L.; Que, L., Jr. *J. Chem. Soc., Chem. Commun.* **1999**, 2161–2162.
- (7) Simaan, A. J.; Boillot, M. L.; Rivière, E.; Boussac, A.; Girerd, J.-J. *Angew. Chem., Int. Ed.* **2000**, *39*, 196–198.
- (8) Hazell, A.; Jensen, K. B.; McKenzie, C. J.; Toftlund, H. *Inorg. Chem.* **1994**, *33*, 3127–3134.
- (9) Kojima, T.; Leising, R. A.; Yan, S.; Que, L., Jr. *J. Am. Chem. Soc.* **1993**, *115*, 11328–11335.
- (10) Chuang, C. L.; Dos Santos, O.; Xu, X.; Canary, J. W. *Inorg. Chem.* **1997**, *36*, 1967–1972.
- (11) Xu, J.; Chuang, C. L.; Canary, J. W. *Inorg. Chim. Acta* **1997**, *256*, 125–128.
- (12) Zahn, S.; Canary, J. W. *Angew. Chem., Int. Ed.* **1998**, *37*, 305–306.
- (13) Harata, M.; Jitsukawa, K.; Masuda, H.; Einaga, H. *Chem. Lett.* **1995**, 61–62.
- (14) Zang, Y.; Kim, J.; Dong, Y.; Wilkinson, E. C.; Appelman, E.; Que, L., Jr. *J. Am. Chem. Soc.* **1997**, *119*, 4197–4205.

- (15) Sugimoto, H.; Sasaki, Y. *Chem. Lett.* **1997**, 541–542.
- (16) Xu, L.; Sasaki, Y.; Abe, M. *Chem. Lett.* **1999**, 163–164.
- (17) Jang, H. G.; Cox, D. D.; Que, L., Jr. *J. Am. Chem. Soc.* **1991**, *113*, 9200–9204.
- (18) 1 OpenMoleN, Interactive Structure Solution, Nonius B.V., Delft, The Netherlands, 1997.

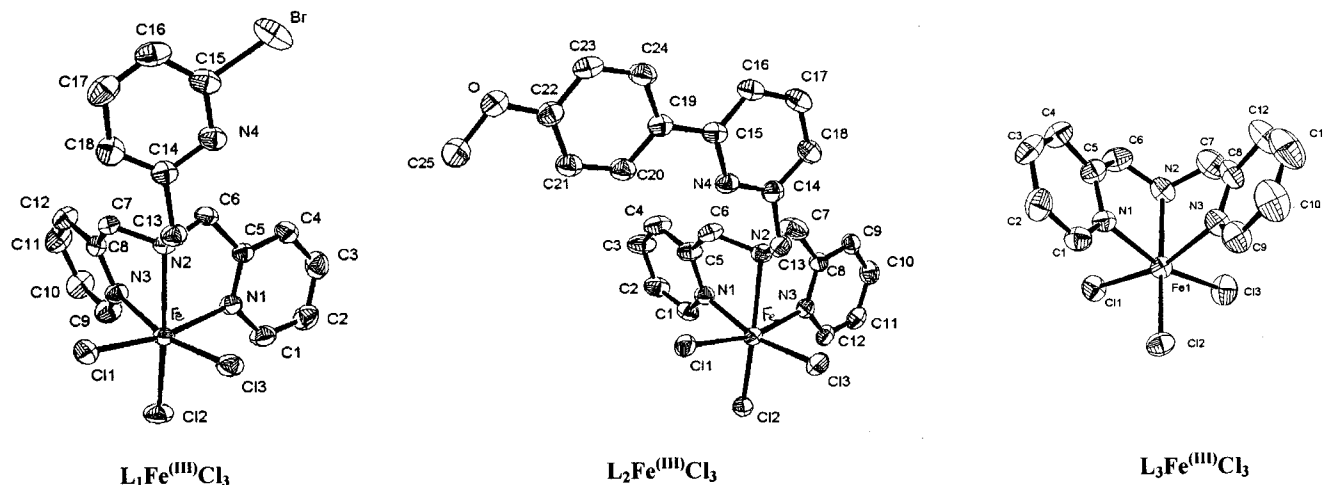


Figure 2. ORTEP diagrams of the $L_n\text{Fe}^{\text{III}}\text{Cl}_3$ complexes.

The structure was solved using direct methods. After refinement of the heavy atoms, a difference Fourier map revealed maximas of residual electronic density close to the positions expected for hydrogen atoms; they were introduced as fixed contributors in structure factor calculations by their computed coordinates ($C-H = 0.95 \text{ \AA}$) and isotropic temperature factors such as $B(H) = 1.3B_{\text{eq}}(C) \text{ \AA}^2$ but not refined. Full least-squares refinements on F_o . A final difference map revealed no significant maxima. The scattering factor coefficients and anomalous dispersion coefficients came respectively from ref 19a and 19b.

Crystal data for $L_1\text{Fe}^{\text{III}}\text{Cl}_3$. Yellow crystals, crystal dimensions $0.40 \times 0.40 \times 0.40 \text{ mm}^3$, $C_{18}H_{17}N_4Cl_3FeBr$, $M = 531.5$, monoclinic, space group $C12/c1$, $a = 20.602(1)$, $b = 14.5887(6)$, and $c = 14.2907(9) \text{ \AA}$, $\beta = 106.227(4)^\circ$, $V = 4124.0(7) \text{ \AA}^3$, $Z = 8$, $D_c = 1.71 \text{ g cm}^{-3}$, $\mu(\text{Mo K}\alpha) = 3.054 \text{ mm}^{-1}$. A total of 4486 reflections were used, $2.5^\circ < \theta < 26.29^\circ$. A total of 2920 independent reflections having $I > 3\sigma(I)$; 244 parameters. Final results: $R(F) = 0.033$, $R_w(F) = 0.048$, $\text{GOF} = 1.004$, maximum residual electronic density = 0.985 e \AA^{-3} .

Crystal Data for $L_2\text{Fe}^{\text{III}}\text{Cl}_3$. Yellow crystals, crystal dimensions $0.23 \times 0.16 \times 0.09 \text{ mm}^3$, $C_{25}H_{24}N_4OCl_3Fe$, $M = 558.7$, monoclinic, space group $P12_1/c1$, $a = 21.9206(6)$, $b = 7.9500(2)$, and $c = 15.2009(4) \text{ \AA}$, $\beta = 109.39(1)^\circ$, $V = 2498.8(4) \text{ \AA}^3$, $Z = 4$, $D_c = 1.48 \text{ g cm}^{-3}$, $\mu(\text{Mo K}\alpha) = 0.951 \text{ mm}^{-1}$. A total of 22038 reflections were used, $2.5^\circ < \theta < 29.55^\circ$. A total of 3369 independent reflections having $I > 3\sigma(I)$; 307 parameters. Final results: $R(F) = 0.039$, $R_w(F) = 0.055$, $\text{GOF} = 1.082$, maximum residual electronic density = 0.365 e \AA^{-3} .

Crystal data for $L_3\text{Fe}^{\text{III}}\text{Cl}_3$. Yellow crystals, crystal dimensions $0.30 \times 0.30 \times 0.30 \text{ mm}^3$, $C_{12}H_{13}N_3Cl_3Fe$, $M = 361.4$, orthorhombic, space group $Pna2_1$, $a = 15.6038(8)$, $b = 8.4742(7)$, and $c = 22.751(1) \text{ \AA}$, $V = 3008.4(6) \text{ \AA}^3$, $Z = 8$, $D_c = 1.60 \text{ g cm}^{-3}$, $\mu(\text{Mo K}\alpha) = 1.528 \text{ mm}^{-1}$. A total of 3483 reflections were used, $2.5^\circ < \theta < 26.29^\circ$. A total of 2203 independent reflections having $I > 3\sigma(I)$; 342 parameters. Final results: $R(F) = 0.028$, $R_w(F) = 0.033$, $\text{GOF} = 1.022$, maximum residual electronic density = 0.228 e \AA^{-3} .

Results and Discussion

The metalation of the ligands is straightforward and requires, as displayed in Figure 1, the stoichiometric addition of an ether solution of anhydrous FeCl_3 to the TPA derivative L_n dissolved in ether ($L_1 = ((2\text{-bromopyridyl)methyl})\text{bis}(2\text{-pyridylmethyl})\text{-amine}$, BrTPA ; $L_2 = (((2\text{-}p\text{-methoxyphenyl})\text{pyridyl})\text{methyl})\text{-bis}(2\text{-pyridylmethyl})\text{amine}$, MeOPhTPA ; $L_3 = \text{bis}(2\text{-pyridylmethyl})\text{amine}$, DPA). Yellow to orange-yellow compounds are thus quantitatively obtained as $L_n\text{Fe}^{\text{III}}\text{Cl}_3$ complexes, which are air stable in the solid state as well as in solution.

Slow diffusion of diethyl ether in acetonitrile solutions of the complexes yielded in each case crystals suitable for X-ray diffraction analysis. As shown in Figure 2, for each complex tridentate coordination is observed, with the substituted pyridine dangling away from the metal for L_1 and L_2 . Consequently, all compounds reported in this paper are neutral molecules.

From a structural point of view, similar features are observed for each compound, i.e., a distorted octahedral geometry with trans ligand angles below 180° , typically for $L_1\text{Fe}^{\text{III}}\text{Cl}_3$, values of $163.02(7)^\circ$ for $\angle\text{Cl}2\text{-Fe-N}2$, $167.56(7)^\circ$ for $\angle\text{Cl}1\text{-Fe-N}1$, and $166.28(7)^\circ$ for $\angle\text{Cl}3\text{-Fe-N}3$. The angles between the chloride ligands are significantly larger than 90° , with values of $97.13(4)^\circ$ for $\angle\text{Cl}1\text{-Fe-Cl}2$, $96.52(4)^\circ$ for $\angle\text{Cl}1\text{-Fe-Cl}3$, and $98.67(3)^\circ$ for $\angle\text{Cl}2\text{-Fe-Cl}3$. The flexibility of the ligand is expressed by the small angles between the nitrogen atoms, with $73.65(9)^\circ$ for $\angle\text{N}2\text{-Fe-N}3$, $77.39(9)^\circ$ for $\angle\text{N}1\text{-Fe-N}2$, and $83.8(1)^\circ$ for $\angle\text{N}1\text{-Fe-N}3$. As is often the case for other already reported $\text{Fe}^{\text{III}}\text{TPA}$ complexes, the $\text{Fe-N}(\text{pyridine})$ bonds (average 2.19 \AA) are shorter than the $\text{Fe-N}(\text{amine})$ bond ($2.281(2) \text{ \AA}$). These bond lengths, listed in Table 1, are consistent with the high spin state of the metal in the complex.

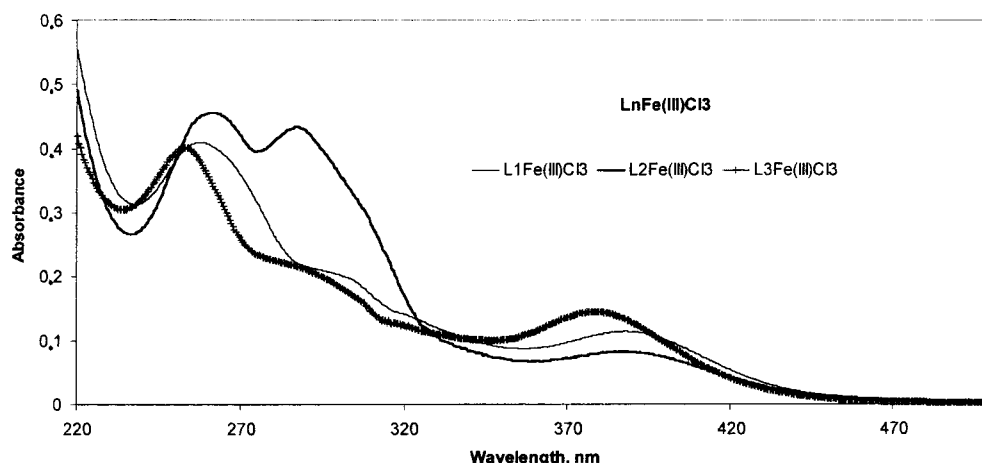
The ferric derivative $[\text{TPAFeCl}_2](\text{ClO}_4)$ has already been structurally characterized, and the ligand displays the usual, tetradentate coordination mode.^{8,9} In our case, tridentate coordination is observed. However, it is likely that the use of other anions, smaller or weakly coordinating, would result in tetradentate coordination of the substituted ligands. Precedents of tridentate coordination with the TPA ligand are known with rhenium and molybdenum complexes and justified by thermodynamic patterns such as trans effects $[(\eta\text{-}3)\text{TPARe}^{\text{V}}\text{OL}]^+$ or decreased π -acceptor capability of the TPA ligand $[(\eta\text{-}3)\text{TPAMo}^0(\text{CO})_3]$.^{14,16} In this study, the choice of chloride ions, which in organic solvents are strongly coordinating, was dictated by the need to obtain complexes displaying excellent criteria of stability in various media. Indeed, the high affinity of the σ donor chloride ions for the iron stabilizes the $L\text{Fe}^{\text{III}}\text{Cl}_3$ form in which the need for an octahedral geometry forces the substituted pyridine to decoordinate. Interestingly, this geometry is retained in solution, as shown by NMR measurements (vide infra).

The UV-visible spectra of the compounds are shown in Figure 3, and their absorption maxima are listed in Table 2. The intense peak in the UV range is broader than and slightly blue-shifted from that in the free ligand and assigned to a ligand-centered $\pi\text{-}\pi^*$ transition. Upon metalation of the ligands, two broad and weak bands appear that we assign as charge-transfer

(19) Cromer, D. T.; Waber, J. T. *International Tables for X-ray Crystallography*, 1974, Vol. IV; Kynoch Press: Birmingham: (a) Table 2.2b, (b) Table 2.3.1.

Table 1. Selected Bond Lengths (Å) and Angles (deg) for the $L_n\text{Fe}^{\text{III}}\text{Cl}_3$ Complexes

$L_1\text{Fe}^{\text{III}}\text{Cl}_3$		$L_2\text{Fe}^{\text{III}}\text{Cl}_3$		$L_3\text{Fe}^{\text{III}}\text{Cl}_3$	
Fe—Cl1	2.293(1)	Fe—Cl1	2.313(2)	Fe—Cl1	2.3076(9)
Fe—Cl2	2.2880(9)	Fe—Cl2	2.279(2)	Fe—Cl2	2.286(1)
Fe—Cl3	2.2867(9)	Fe—Cl3	2.288(2)	Fe—Cl3	2.296(1)
Fe—N1	2.166(3)	Fe—N1	2.191(4)	Fe—N1	2.185(3)
Fe—N2	2.281(2)	Fe—N2	2.211(5)	Fe—N2	2.300(3)
Fe—N3	2.220(3)	Fe—N3	2.177(5)	Fe—N3	2.176(3)
Cl1—Fe—Cl2	97.13(4)	Cl1—Fe—Cl2	97.81(7)	Cl1—Fe—Cl2	98.07(4)
Cl1—Fe—Cl3	96.52(4)	Cl1—Fe—Cl3	98.90(7)	Cl1—Fe—Cl3	97.92(4)
Cl1—Fe—N1	167.56(7)	Cl1—Fe—N1	87.2(1)	Cl1—Fe—N1	87.61(7)
Cl1—Fe—N2	90.19(7)	Cl1—Fe—N2	90.4(1)	Cl1—Fe—N2	90.41(7)
Cl1—Fe—N3	92.20(8)	Cl1—Fe—N3	162.8(1)	Cl1—Fe—N3	164.81(8)
Cl2—Fe—Cl3	98.67(3)	Cl2—Fe—Cl3	98.88(7)	Cl2—Fe—Cl3	97.65(4)
Cl2—Fe—N1	94.70(8)	Cl2—Fe—N1	94.2(1)	Cl2—Fe—N1	93.58(8)
Cl2—Fe—N2	163.02(7)	Cl2—Fe—N2	167.5(1)	Cl2—Fe—N2	164.73(8)
Cl2—Fe—N3	90.71(7)	Cl2—Fe—N3	93.3(1)	Cl2—Fe—N3	93.11(8)
Cl3—Fe—N1	85.47(8)	Cl3—Fe—N1	164.6(1)	Cl3—Fe—N1	166.63(8)
Cl3—Fe—N2	95.68(7)	Cl3—Fe—N2	89.2(1)	Cl3—Fe—N2	93.71(8)
Cl3—Fe—N3	166.28(7)	Cl3—Fe—N3	92.2(1)	Cl3—Fe—N3	90.71(8)
N1—Fe—N2	77.39(9)	N1—Fe—N2	76.6(2)	N1—Fe—N2	74.0(1)
N1—Fe—N3	83.8(1)	N1—Fe—N3	78.9(2)	N1—Fe—N3	81.4(1)
N2—Fe—N3	73.65(9)	N2—Fe—N3	76.7(2)	N2—Fe—N3	76.5(1)

**Figure 3.** Electronic absorption spectra of the $L_n\text{Fe}^{\text{III}}\text{Cl}_3$ complexes in acetonitrile (concentration: $L_1\text{Fe}^{\text{III}}\text{Cl}_3$, 0.282 mmol; $L_2\text{Fe}^{\text{III}}\text{Cl}_3$, 0.236 mmol; $L_3\text{Fe}^{\text{III}}\text{Cl}_3$, 0.299 mmol).**Table 2.** Absorption Maxima for the $L_n\text{Fe}^{\text{III}}\text{Cl}_3$ Complexes

complex	wavelength, λ_{max} , nm (ϵ , $10^{-3} \text{ mmol}^{-1} \text{ cm}^2$), CH_3CN , rt
$L_1\text{Fe}^{\text{III}}\text{Cl}_3$	257 (14.70) 301 (7.14) 390 (4.05)
$L_2\text{Fe}^{\text{III}}\text{Cl}_3$	261 (20.40), 287 (19.40) 308 (sh.) 385 (3.69)
$L_3\text{Fe}^{\text{III}}\text{Cl}_3$	253 (13.40) 295 (6.64) 378 (4.82)

transitions from the coordinated chloride to the metal. In the visible range, the values of 378.0 nm ($L_3\text{Fe}^{\text{III}}\text{Cl}_3$), 384.5 nm ($L_2\text{Fe}^{\text{III}}\text{Cl}_3$), and 389.5 nm ($L_1\text{Fe}^{\text{III}}\text{Cl}_3$) are not far from that reported for the $\text{TPAFe}^{\text{III}+}$ cation ($\lambda_{\text{max}} = 382 \text{ nm}$), thus indicating for all complexes a similar ligand field around the metal.⁹

The ^1H NMR spectra of the $L_n\text{Fe}^{\text{III}}\text{Cl}_3$ complexes look very similar and differ from those of the already reported TPA ferric monomers in which the tripod acts as a tetradentate ligand.^{8,9,17} The spectra are dominated in the paramagnetic region by three very broad resonances, listed in Table 3. For $L_2\text{Fe}^{\text{III}}\text{Cl}_3$ for instance, as shown in Figure 4, they appear at $\delta = 105, 91,$ and 52 ppm . On the basis of the integrals and T_1 relaxation times, we assign the downfield signals to the β and β' protons of the coordinated pyridines. The middle field shifted signal is extremely broad and, although less shifted than the β protons, is assigned to the α protons of the coordinated arms with the smallest observed relaxation time. In the diamagnetic region, the sharp resonance at $\delta = 11.5 \text{ ppm}$ is assigned to the γ -pyridyl

Table 3. ^1H NMR Chemical Shifts and T_1 Relaxation Times for the $L_n\text{Fe}^{\text{III}}\text{Cl}_3$ Complexes^a

Complex	Chemical shift, δ , ppm, CD_3CN , R.T. (T_1 , μs)							
	β, β', α	β_u	γ	<i>o</i> -phen	μ -phen	γ_u	<i>OCH</i> ₃	
$L_1\text{Fe}^{\text{III}}\text{Cl}_3$	104 (84)	90 (114)	44 (68)	14.0 (3478)	11.5 (1373)		4.6 (6520)	
$L_2\text{Fe}^{\text{III}}\text{Cl}_3$	105 (88)	91 (99)	52 (76)	14.6 (2608)	11.5 (1272)	8.1 (1862)	7.0 (5794)	
$L_3\text{Fe}^{\text{III}}\text{Cl}_3$	104 (84)	87 (83)	33 (85)		12.5 (1346)			

^a $\beta, \beta', \alpha, \gamma$: common features. β_u, γ_u (dark gray): uncoordinated pyridyl arm. *o*-, *m*-phen, *OCH*₃ (light gray): methoxyphenyl substituent.

protons of the coordinated pyridine. A comparison of NMR data of TPA derivatives $L_1\text{Fe}^{\text{III}}\text{Cl}_3$ and $L_2\text{Fe}^{\text{III}}\text{Cl}_3$ with that of $L_3\text{Fe}^{\text{III}}\text{Cl}_3$ indicates that the only difference is the presence in the former two complexes of extra signals in the diamagnetic region, with two of them found at 14.0 (14.6 for $L_2\text{Fe}^{\text{III}}\text{Cl}_3$) and 4.6 (5.0 for $L_2\text{Fe}^{\text{III}}\text{Cl}_3$) ppm. We assign these signals to the β - and γ -pyridyl protons of the pyridyl arm obviously missing in $L_3\text{Fe}^{\text{III}}\text{Cl}_3$. Thus: (i) all compounds display a similar environment at the paramagnetically shifted sites, indicating an identical symmetry and coordination mode; (ii) because of the small shifts

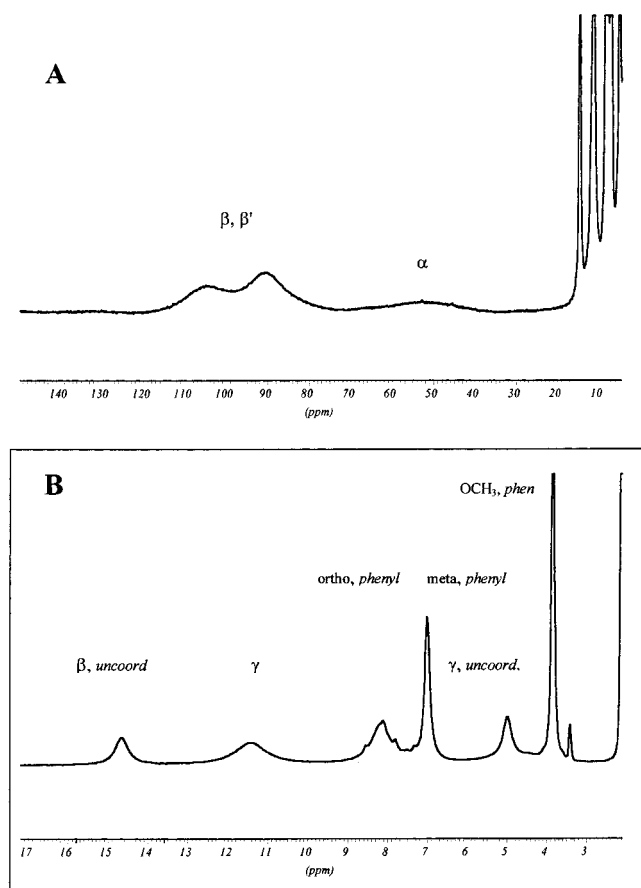


Figure 4. ^1H NMR spectrum of $\text{L}_2\text{Fe}^{\text{III}}\text{Cl}_3$, CD_3CN , room temperature: trace A, paramagnetic region; trace B, diamagnetic region.

and longer relaxation times, the two above-mentioned extra signals indicate that the substituted pyridyl arm remains uncoordinated. With $\text{L}_2\text{Fe}^{\text{III}}\text{Cl}_3$, additional evidence of the noncoordination of the substituted pyridyl arm arises from the observation of resonances of the phenyl and methoxy groups at $\delta = 8.1$, 7.0, and 3.9 ppm with long relaxation times. Thus, we demonstrate that the structure as observed from the solid state is retained in solution.

In the paramagnetic region the T_1 relaxation times are very short, ranging from 60 to 120 μs . This supports a high spin state, $S = 5/2$, for the iron in these complexes. ^1H NMR data have already been reported on the ferric high spin monomers $\text{FeCl}_2(\text{TPA})^+$, ClO_4^- and $\text{Fe}(\text{DBC})(\text{TPA})^+$, BPh_4^- .^{9,17} In these compounds, the resonances appear at lower fields (245, 165, 137, 112, 90 ppm and 196, 116, 92, 90 ppm, respectively) but the T_1 relaxation times range from 100 to 1000 μs . The α -protons signal also display the shortest relaxation times but, in contrast to our compounds, are more shifted than the β -ones. Another difference in our compounds is the absence of any signals, either broad and shifted, in the diamagnetic region assigned to the methylene protons. The reasons for these differences are as yet unclear. In our compounds, which are neutral molecules with only two coordinated pyridines, the nuclear relaxation times are short, which might reflect a higher spin density delocalized over the ligand. Also likely is that the broadness of the bands might arise from a longer electronic spin–lattice relaxation time. Extensive spectroscopic studies addressing this point will be reported in a forthcoming article.

In conclusion, we have shown that α -monofunctionalization of TPA ligands with bulky groups induces tridentate coordination in FeCl_3 derivatives. The uncoordinated arm is the substituted pyridine, and comparison of NMR data with those of the bis(pyridylmethyl)amine parent complex, whose crystal structure is also reported, indicates that this geometry is retained in solution. These high spin compounds are very stable, and the presence of potentially reactive pyridine at their periphery, together with a metal protecting the tertiary amine, opens the way to further use of these complexes in synthetic strategies.

Acknowledgment. The authors are indebted to Prof. J. Fischer, Dr. A. De Cian, Mrs. N. Gruber, and the Service Commun de Rayons X, Faculté de Chimie, Université Louis Pasteur, for the X-ray structural determinations. Financial support by the CNRS and the ULP is gratefully acknowledged.

Supporting Information Available: Crystallographic files in CIF format for the three reported structures. This material is available free of charge via the Internet at <http://pubs.acs.org>.

IC001339P